J. Astrophys. Astr. (1983) **4**, 175–182

Reflection Effect in Close Binaries. IV. Limb Darkening of the Reflected Radiation Incident from an Extended Surface of the Secondary

A. Peraiah and M. Srinivasa Rao *Indian Institute of Astrophysics, Bangalore 560034*

Received 1983 January 24; accepted 1983 July 6

Abstract. The law of limb darkening has been calculated when the atmosphere of the primary component is illuminated by the extended surface of the secondary component in a binary system. The specific intensities calculated at infinity show marked changes when the plane-parallel approximation is replaced by the assumption of spherical symmetry. The middle portions of the illuminated surface reflect maximum radiation while the innermost and outermost layers show lesser amount of reflected radiation.

Key words: reflection effect—limb darkening

1. Introduction

It is customary to assume a law of limb darkening (see Kitamura 1954; Kopal 1959; Peraiah 1970) which is based on blackbody considerations. It is necessary to actually calculate the distribution of radiation field and then derive the law of limb darkening. In paper 2 of this series, the law of limb darkening was calculated as observed at infinity. It was assumed that the incident radiation was emitted by a point source. The self-radiation of the component had been estimated by using plane-parallel and spherically-symmetric approximations for the sake of comparison. Large differences occur in the radiation received at infinity when the above two approximations are employed. This encourages one to proceed further to investigate the radiation field received at infinity when the incident radiation comes from an extended surface of the secondary instead of a point source.

2. Computational procedure

The geometry of the model is shown in Fig. 1(a). O and O′ are the centres of the primary and secondary respectively. The atmosphere of the primary is divided into several shells. We would like to calculate the effect of irradiation from the secondary on the

distribution of radiation field in the part of the atmosphere of the primary facing the secondary. We have considered a set of rays along the line of sight and tangential to the shell boundaries at points where the axis OO′ intersect them. We estimate the radiation field at points such as P where the parallel rays meet the shell boundaries. The radiation field at P is calculated by estimating the source function at P due to the radiation incident at P from the surface SW of the secondary facing the primary. We have selected a number of rays from SW incident on the atmosphere and entering the surface at points such as T, τ *etc.* We intend to calculate the ray paths PT, Pτ *etc.*, and optical depths along these rays. The segments such as Pτ in $\underline{|\mathrm{TPT}_1}$ are given by

$$\mathrm{P}\tau = \mathrm{OP}\left(A\frac{B'}{B} + A'\right) \tag{1}$$

where

$$B = \frac{\mathrm{OP}}{\mathrm{OT}}A, \qquad B' = (1-B^2)^{\frac{1}{2}},$$

$$A = \xi\eta' - \xi'\eta, \qquad A' = (1-A^2)^{\frac{1}{2}},$$

$$\eta = \sin E = \frac{\mathrm{SE}}{\mathrm{PE}}, \qquad \eta' = \cos E,$$

$$\xi = abc + a'b'c + a'bc' - ab'c', \qquad \xi' = (1-\xi^2)^{\frac{1}{2}},$$

$$a = \mathrm{OQ/OP}, \qquad a' = (1-a^2)^{\frac{1}{2}},$$

$$b = \mathrm{PS/O'P}, \qquad b' = (1-b^2)^{\frac{1}{2}},$$

$$c = \mathrm{PQ/O'P}, \qquad c' = (1-c^2)^{\frac{1}{2}}.$$

Similarly the segments such as Pτ in $\underline{|\mathrm{T}_1\mathrm{PT}_2}$ are given by

$$\mathrm{P}\tau' = \mathrm{OP}\left[\mu\left(\frac{s'}{s}\right) + \mu'\right], \tag{2}$$

where

$$\mu = \nu'\Delta + \Delta'\nu, \qquad \mu' = (1-\mu^2)^{\frac{1}{2}},$$

$$s = \frac{\mathrm{OP}}{\mathrm{OT}}\mu, \qquad s' = (1-s^2)^{\frac{1}{2}},$$

$$\nu = \frac{\mathrm{WE}'}{\mathrm{PE}'}, \qquad \nu' = (1-\nu^2)^{\frac{1}{2}},$$

$$\mathrm{PE}' = (\mathrm{PW}^2 + \mathrm{WE}'^2)^{\frac{1}{2}}, \qquad \Delta = \xi(1-2\delta^2) - 2\xi'\delta\delta',$$

$$\Delta' = (1-\Delta^2)^{\frac{1}{2}}, \qquad \delta = \frac{\mathrm{SO}'}{\mathrm{PO}'},$$

$$\delta' = (1-\delta^2)^{\frac{1}{2}}.$$

For a given density distribution, we can calculate the optical depth along the segments such as Pτ and Pτ'. Using these optical depths, the specific intensities and source

functions at the point P due to irradiation from the secondary can be calculated. The boundary conditions and the method of calculation have been described in paper III of this series. We solve the equation of radiative transfer in spherical symmetry and obtain the source function S_S due to self radiation. Here we have calculated the optical depth according to $1/r^2$ law of variation of electron density and assumed isotropic scattering by electrons. The total source function S_T is the sum of the source functions due to self radiation S_S and irradiation S_I:

$$S_T = S_S + S_I. \tag{3}$$

We thus calculate the set of source functions at the points of intersection of the ray parallel to the line of sight and the shell boundaries. These source functions are used to calculate the emergent specific intensities at infinity by using the formula

$$I_{n+1}(r) = I_0(n) \exp(-\tau)^+ \int_0^{\tau} S_T(t) \exp[-(\tau - t)]dt, \tag{4}$$

where $I_n(r)$ corresponds to the specific intensity of the ray passing between shell numbers n and $n+1$ corresponding to perpendicular radial distance r, along the axis OO'. $I_0(n)$ corresponds to the incident intensity at the boundary of the shell and τ is the optical depth in the sector along the ray path. The source function $S_T(t)$ is calculated by linear interpolation between $S_T(n)$ and $S_T(n+1)$. The specific intensity at the boundary of each shell is calculated by using Equation (4).

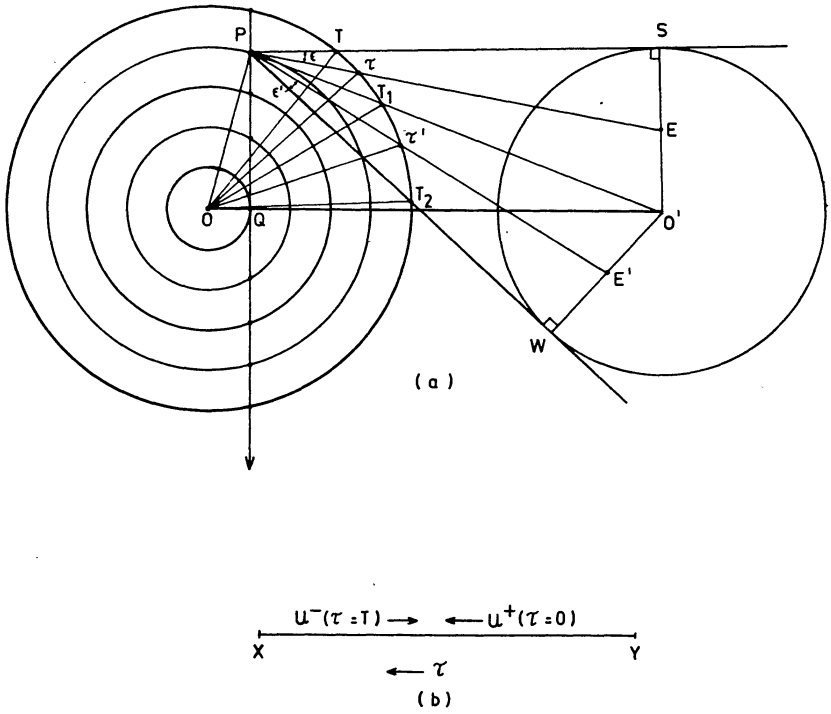

Figure 1. (a) Schematic diagram of the model of reflection of radiation from the extended surface of the secondary. (b) Schematic diagram of the Rod model. u^+ and u^- are the specific intensities in the opposite directions.

3. Results and discussion

In Fig. 1(a), we have given the schematic diagram of the model. We have divided the atmosphere into 25 shells. The line of sight is in the direction of PQ. We have calculated the source functions at the points where PQ meets the shell boundaries. It must be noted that the configuration shown in Fig. 1(a) in this paper is different from Fig. 1(a) of Paper 3. We are considering here the radiation along the line of sight whereas in the earlier case, we calculated the radiation field along the radius vector. Therefore one need not look for similarities. In Fig. 1(b) we show the rod model. In Fig. 2, the source functions due to reflection are plotted. Shell number 1 has its inner boundary at the point Q; the outer boundary of the shell number 25 coincides with that of the outer boundary of the atmosphere. We have assumed a $1/r^2$ law of density variation, with a density of 10^{13} cm^{-3} at Q. The total radial optical depth reaches a maximum of 4; along the line of sight it varies between 0 and 5 from outermost layer to the innermost layer at Q, depending upon the perpendicular distance of the ray path from O along the axis OO′. The source functions S_I at points of intersection of the axis OO′ and shell boundaries are plotted in Fig. 2(a), for different values of I, the ratio of the radiations of

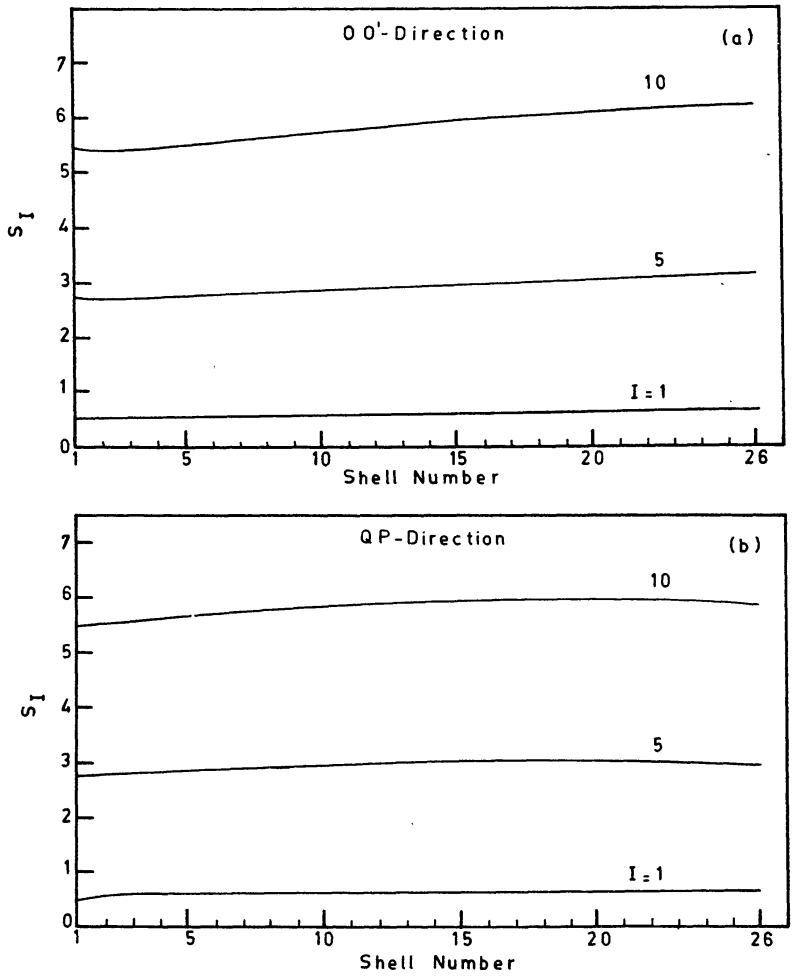

Figure 2. The source functions S_I due to reflection in (a) OO′ direction and (b) QP direction. S_I is given in arbitrary units.

the two components (see Paper 3). We notice that the source functions are almost linear and increase with the shell numbers, *i.e.*, towards the secondary component from whose surface the primary is receiving the incident radiation. This can be understood easily on physical grounds. However, the increase is not as big as one expects because of the fact that the density falls as $1/r^2$ towards the outer layers of the atmosphere. The source functions S_I (due to incident radiation from the secondary component) along the line of sight QP (tangent to the star's surface) are plotted against the shell numbers in Fig. 2(b). The behaviour of S_I here, is slightly different from that of Fig. 2(a). It increases slowly towards P and then starts falling. This can be understood on the basis that the incident radiation, on reaching points such as P which are away from the centre of the star, is weakened by the cosine factor.

Compare Fig. 2 with Fig. 3 of Paper 3. Here we have plotted the source function due to irradiation only, whereas in the earlier case, we had plotted the total source function

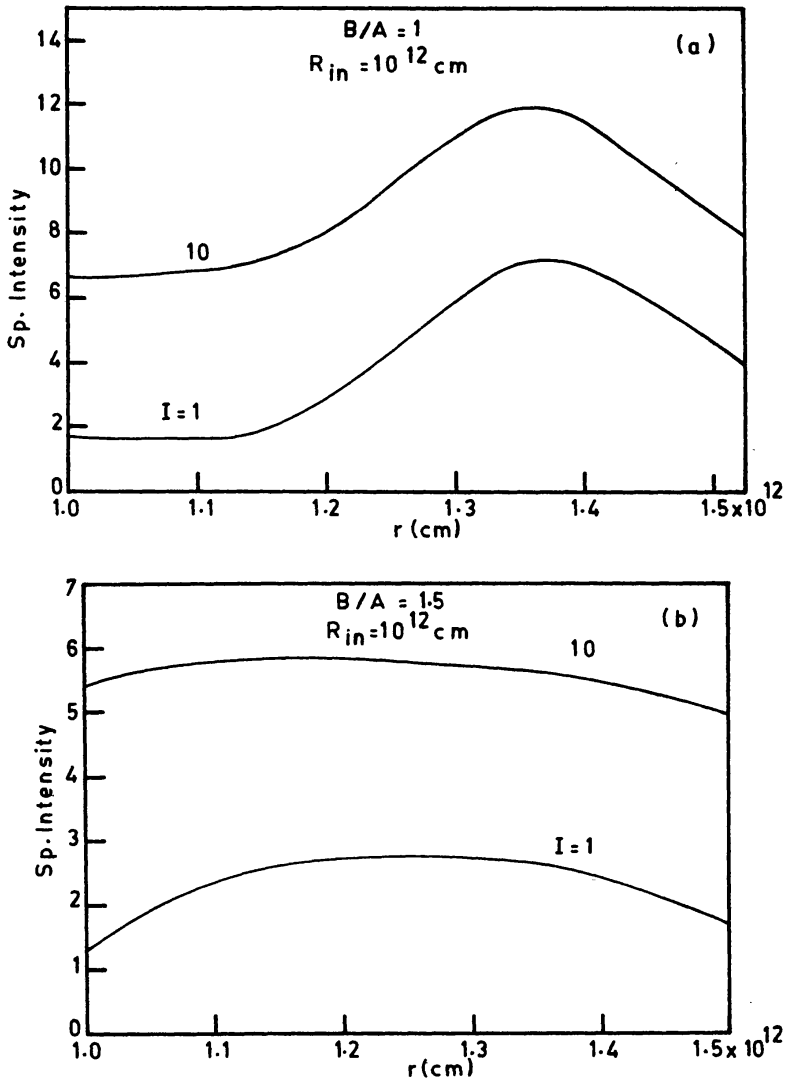

Figure 3. Variation of specific intensity from centre to limb is given in arbitrary units with (a) plane-parallel geometry ($B/A = 1$) and (b) spherical geometry ($B/A = 1.5$), where B and A are the outer and inner radii of the atmosphere ($R_{in} = 10^{12}$ cm).

$(S_I + S_S)$. The specific intensity along the line of sight is given in Figs 3–5. The results given in Fig. 3 refer to those of plane-parallel (a) and spherically-symmetric (b) approximations. This means that the source function S_S due to self-radiation is calculated using the above two geometrical stratifications, while the source function S_I due to incident radiation remains the same in both the cases. The source function in

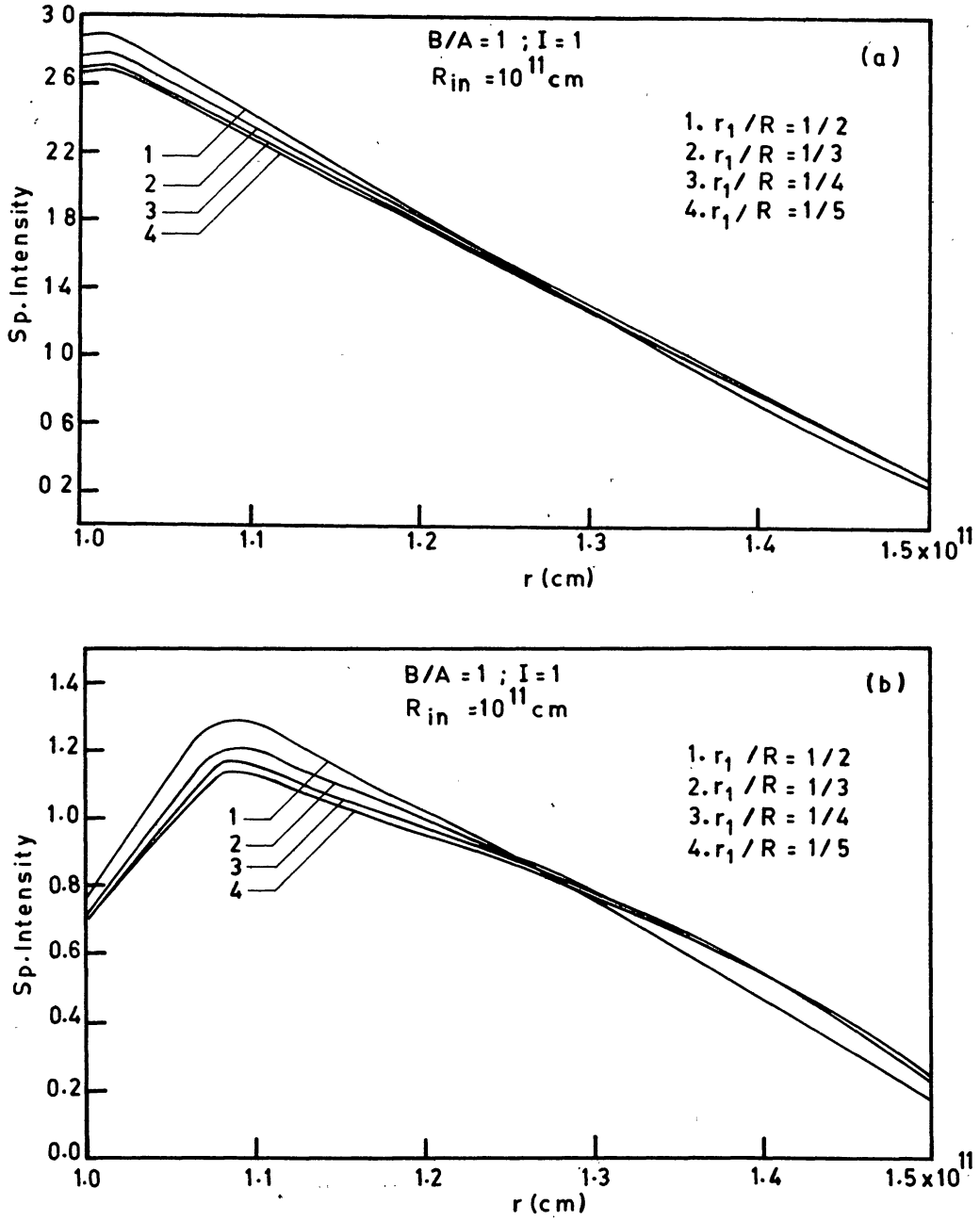

Figure 4. Variation of specific intensities from centre to limb in (a) plane-parallel geometry and (b) spherically symmetric geometry, for $I = 1$ and $R_{in} = 10^{11}$ cm. The results are given for different values of r_1/R, where r_1 is the outer radius of the star and R is the separation between the centres of the two components.

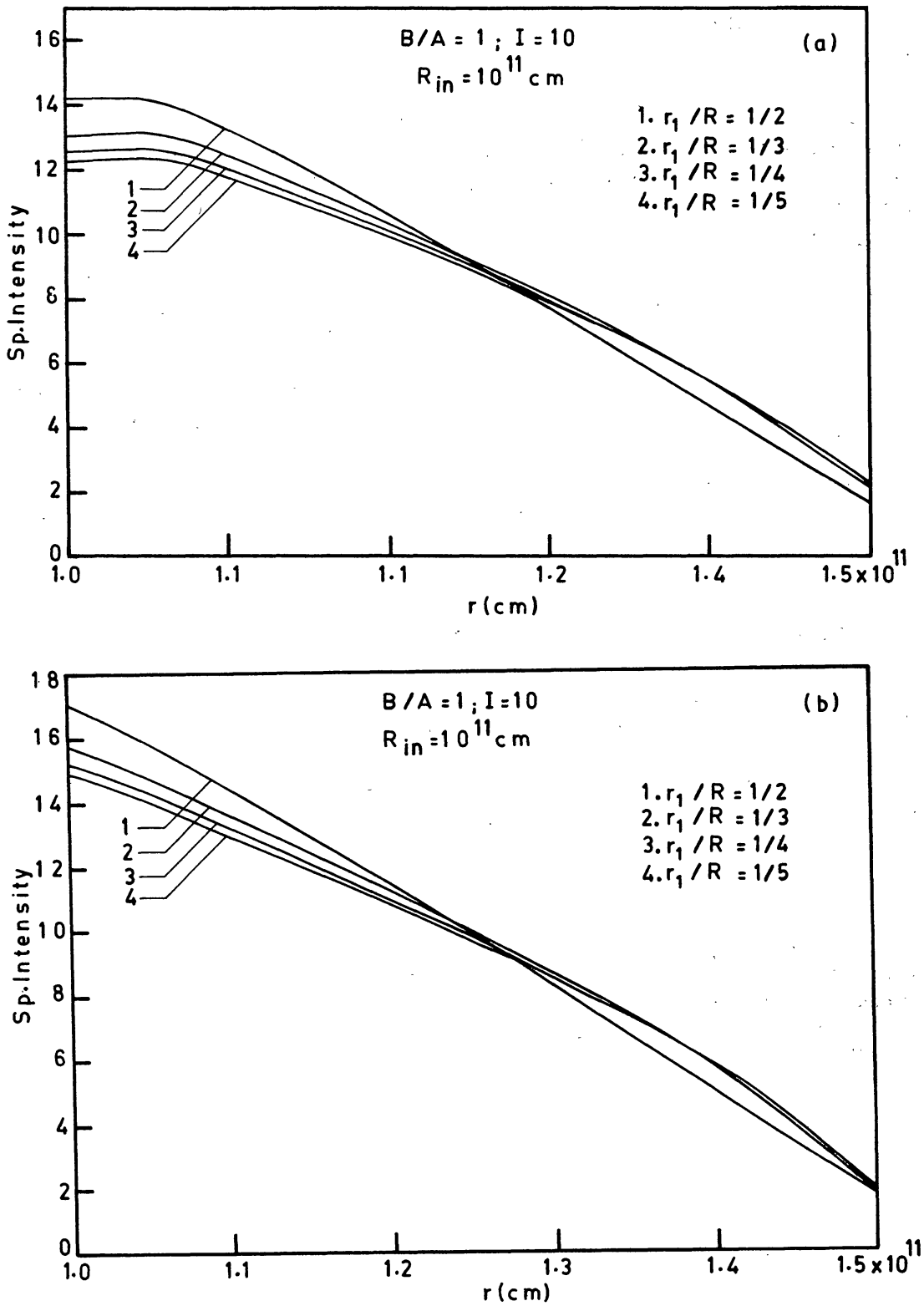

Figure 5. Variation of specific intensities from centre to limb in (a) plane-parallel geometry and (b) spherically symmetric geometry, for $I = 10$ and $R_{in} = 10^{11}$ cm.

plane-parallel approximation is obtained from the solution of the radiative transfer equation without the term,

$$\frac{1}{r}\frac{\partial}{\partial\mu}\left[(1-\mu^2)u(r,\mu)\right].$$

We have calculated the optical depth in spherical and plane-parallel approximations by assuming the same electron density distribution. We have considered an atmosphere whose thickness is one-half of the stellar radius in calculating the source function due to self radiation. The results given in Fig. 3(a) and (b) show different types of variations in the specific intensities from $r = r_{in}$ to $r = r_{out}$. In plane-parallel stratification, the intensities remain constant until some point and then reach a maximum at $r \simeq 1.35 \times 10^{12}$ cm. From here onwards, the intensities fall as one approaches the outer surface of the atmosphere. In the case of spherical geometry, the intensities increase slightly and then decrease towards the outer surface. The law of variation of the intensities from centre to limb is different in the two approximations. Although the extension of the atmosphere is only one half of the stellar radius, the differences are quite large. Therefore, one must always use the assumption of spherical symmetry even when the atmosphere is small compared to the stellar radius. In Fig. 4, we have plotted the variation of specific intensities from centre to limb for $R_{in} = 10^{11}$ cm, $I = 1$, for various values of r_1/R, where r_1 is the outer radius of the star and R is the distance between the centres of the two stars. In plane-parallel approximation, the law of variation of specific intensities is almost linear and falls rapidly towards the surface, whereas in the case of spherical symmetry, the specific intensities reach a maximum and then fall. The results given in Fig. 5 show a trend similar to those given in Fig. 4. The law of limb darkening does not seem to depend much on the ratio r_1/R.

We have shown in this paper that the law of variation of radiation from centre to limb depends considerably on whether one considers plane-parallel or spherically symmetric geometry and also on the distribution of electron density.

References

Kitamura, M. 1954, *Publ. astr. Soc. Japan*, **5**, 114.
Kopal, Z. 1959, *Close Binary Systems*, John Wiley, New York.
Peraiah, A. 1970, *Astr. Astrophys.*, **7**, 473.
Peraiah, A. 1983, *J. Astrophys. Astr.*, **4**, 11 (Paper 2).
Peraiah, A. 1983, *J. Astrophys. Astr.*, **4**, 151 (Paper 3).

J. Astrophys. Astr. (1983) **4**, 183–189

Reflection Effect in Close Binaries. V. Effects of Reflection on Spectral Line Formation

A. Peraiah and M. Srinivasa Rao *Indian Institute of Astrophysics, Bangalore 560034*

Received 1983 February 9; accepted 1983 July 6

Abstract. The effects of reflection on the formation of spectral lines is investigated. We have assumed a purely scattering atmosphere and studied how the equivalent widths change due to irradiation from the secondary. Generally, the flux in the lines is increased at all frequency points, the cores of the lines receiving more flux than the wings. Moreover, the proximity of the secondary component changes the equivalent widths considerably. The further away the secondary is from the primary the higher are the equivalent widths.

Key words: reflection effect—spectral line formation

1. Introduction

We have investigated so far (Peraiah 1982: Paper 1; Peraiah 1983a: Paper 2; Peraiah 1983b: Paper 3; Peraiah & Rao, 1983: Paper 4), how the irradiation from the secondary component changes the radiation field in the atmosphere of the primary. This has been done assuming a purely scattering atmosphere in a monochromatic situation. This also helps in proper understanding of the observed total light that is emitted by the system. Napier & Ovenden (1970) tried to explain by means of reflection effect, the correlation between the velocity amplitudes of individual absorption lines and their wavelengths observed in 57 Cygni. However, they could not succeed in this, because of the fact that they did not use a detailed calculation of the radiation field modified by the incidence of the external radiation. There is another important observational aspect in close binaries that must be understood clearly – the change in the equivalent widths of the lines between eclipses. The spectral lines in 12 Lacertae undergo a periodic variation in width, the lines being wide and diffuse at periastron and sharper and narrower at apastron (Young 1922). There are several explanations put forward for explaining this phenomenon. However, the fact that the lines become wide and diffuse at periastron point, indicates that mutually reflected radiation increases the flux in the lines because of the proximity of the two components. Therefore, we shall study in the present paper how reflection affects the spectral lines. We shall assume a purely scattering medium.

2. Computational procedure and discussion of the results

The procedure to calculate the lines is similar to that used to calculate the radiation in the scattering medium due to electrons. The radiative transfer equation which is employed in calculating the source function due to self-radiation is written as (see Grant & Peraiah 1972),

$$\mu \frac{\partial I(x,\mu,r)}{\partial r} + \frac{1-\mu^2}{r} \frac{\partial I(x,\mu,r)}{\partial \mu} = K_L(r)[\beta + \phi(x)][S_S(x,r) - I(x,\mu,r)]. \quad (1)$$

Here, $I(x, \mu, r)$ is the specific intensity of the ray making an angle $\cos^{-1}\mu$ with the radius vector r. x is the standardised frequency given by

$$x = (\nu - \nu_0)/\Delta_S,$$

where Δ_S is a standard frequency interval. $S_S(x,r)$ is the source function at r for the frequency x. We have considered a Doppler profile for $\phi(x)$. $K_L(x)$ is the absorption coefficient at the centre of the line per unit interval of Δ_S. β is the ratio of the opacity in the continuum to that in the line per unit frequency interval. The procedure of solving the equation is described in Grant and Peraiah (1972). We have set β equal to zero. We have assumed a purely scattering medium due to electrons and used Thomson scattering coefficient in calculating the optical depth. We have assumed that the continuum radiation is supplied by the star. We specify the quantity $I(\tau = T, \mu, x)$ where T is the maximum optical depth (measured from outside towards the centre of the star).

The calculation of the source function due to irradiation S_I, is described in Paper 4. The geometry is described in Fig. 1. O is the centre of the component whose atmosphere is facing the secondary with its centre at O′. The atmosphere of O is divided into several shells of equal geometrical thickness. We consider rays parallel to the line of sight. Each ray is drawn as tangent to the shell boundary where this boundary meets the OO′ axis. This means that we set the orbital plane of the binary to be perpendicular to the line of sight. We compute the total source functions at points such as P where the rays intersect

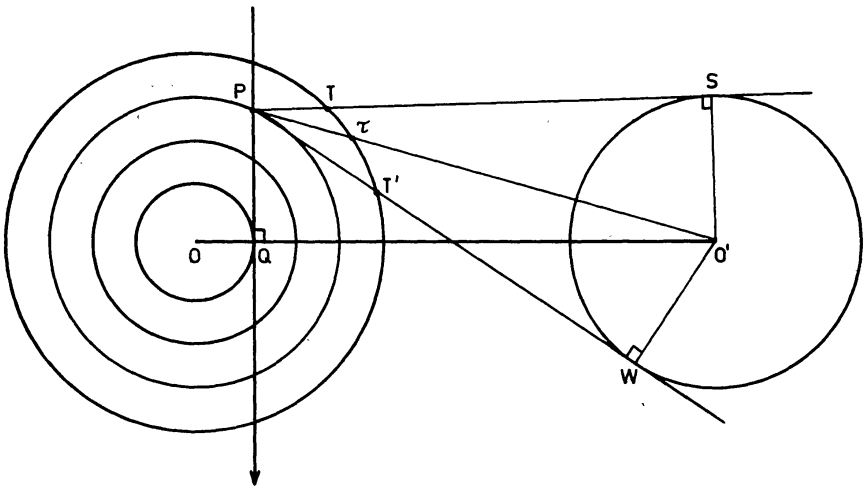

Figure 1. Schematic diagram of the model.

the shell boundaries. The total source functions S_T is given by

$$S_T = S_I + S_S. \tag{2}$$

The radius of the primary is taken to be 10^{12} cm and the atmosphere is taken as half of the stellar radius. The primary and the secondary components are assumed to have equal radii. We have assumed an electron density of 10^{13} cm^{-3} at the innermost radius of the atmosphere and let it vary as $1/r^2$. The source function due to reflection changes considerably whether we go along OO′ direction or along QP direction. The quantity S_S is the same along the boundary of a given shell because of spherical symmetry although this will be different for different shells. We have plotted the total source function with respect to the shell number. We have also studied the effect of proximity of the secondary component to the primary in terms of the parameter r_1/R where r_1 is the radius of the primary and R = OO′. Another quantity we have used is I, the ratio of the luminosities of the primary and the secondary (see Paper 2). The total source function S_T is plotted in Figs 2 and 3. In Fig. 2(a), S_T is plotted for the OO′ direction with $I = 1$ and $r_1/R = 1/2$, 1/3, 1/4, 1/5. In all these figures, shell numbers 1 and 26

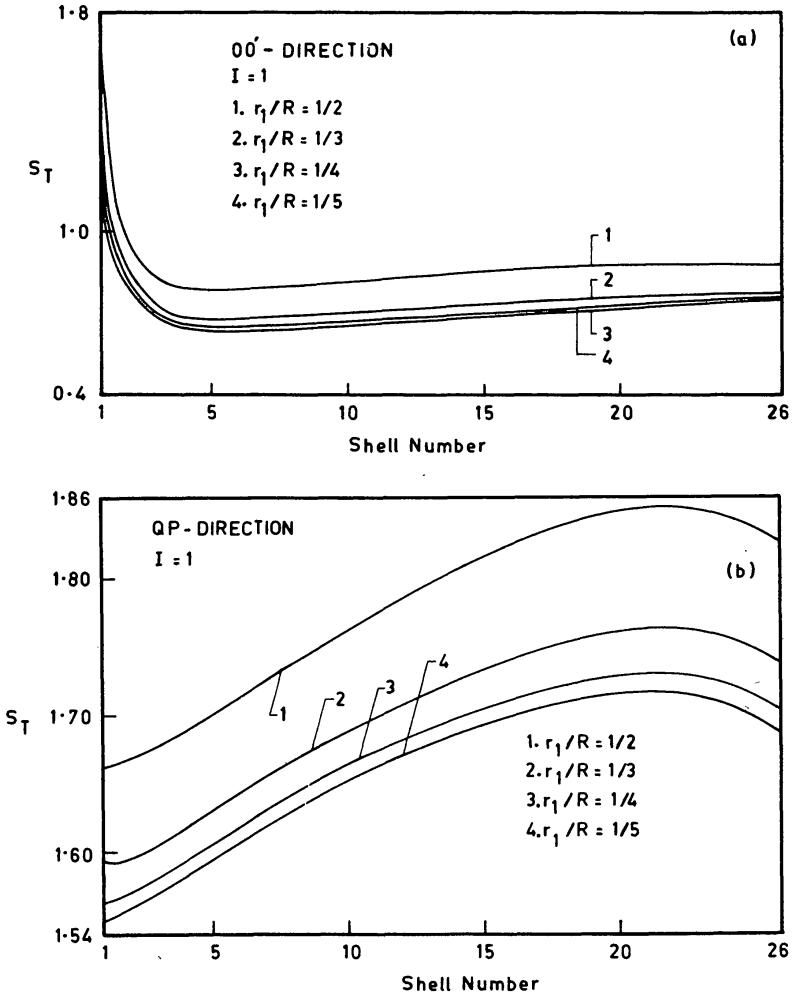

Figure 2. The total source function S_T corresponding to different shell numbers is plotted for $I = 1$ along (a) OO′ direction and (b) QP direction. S_T is given in arbitrary units.

correspond to the innermost and outermost radii of the atmosphere respectively. The source functions have their maxima at shell number 1 and fall rapidly before they reach shell number 4 where they reach the minimum values and then start to increase slowly towards shell number 25. The increase is not as fast as the fall at the innermost shells simply because the electron density falls as $1/r^2$; as soon as the source function reaches a minimum value, the irradiation from the secondary takes over and the source function starts increasing. As the number density of electrons falls towards the outer radius, the amount of scattered radiation also falls. Therefore, the increase in the source function is not steep. The differences introduced into S_T, by the changes in the parameter r_1/R are not very large as can be seen from the figure. The curves corresponding to the last two cases (*i.e.*) $r_1/R = 1/4$ and $1/5$ merge together. In Fig. 2(b), we have plotted S_T with respect to shell number along the line of sight, *i.e.* along QP, where OQ is the innermost radius of the atmosphere. The behaviour of S_T along QP

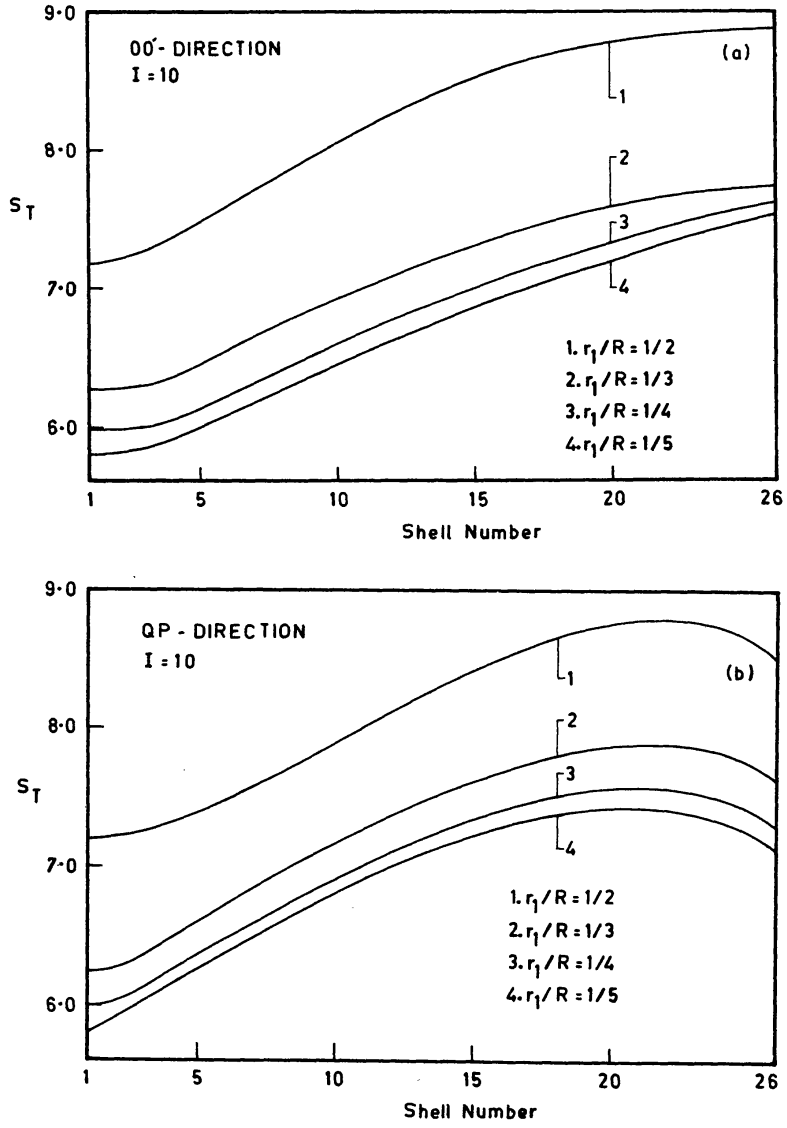

Figure 3. The total source function S_T corresponding to different shell numbers is plotted for $I = 10$ along (a) OO′ direction and (b) QP direction, S_T is given in arbitrary units.

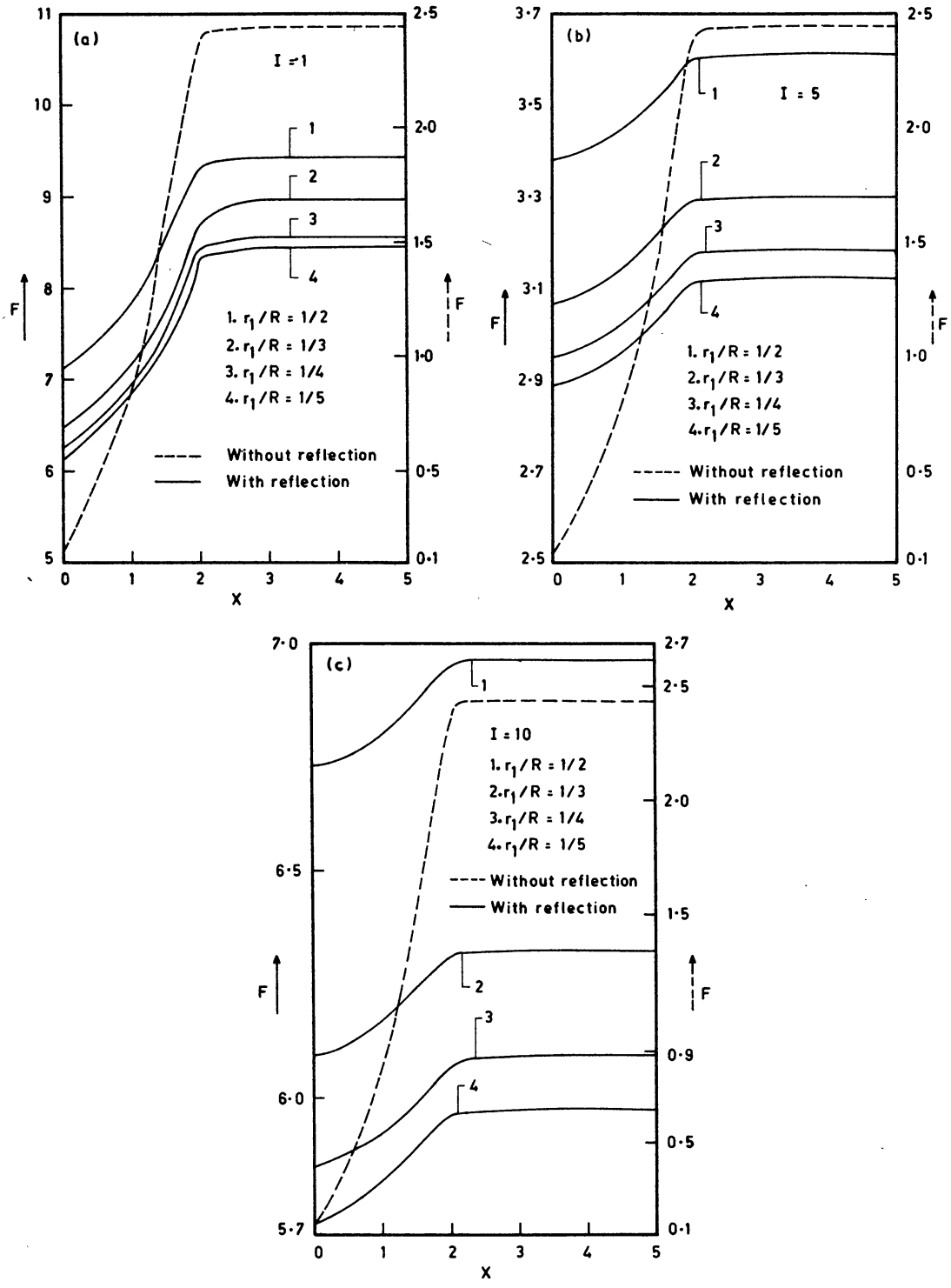

Figure 4. The flux profiles of lines are given in arbitrary units for (a) $I = 1$, (b) $I = 5$ and (c) $I = 10$. The dashed line represents the flux profile without irradiation and its ordinate scale is given on the right-hand side. The continuous lines represent the flux profiles with irradiation, whose scale is given on the left-hand side.

direction is completely different from S_T along OO′ direction. The source functions start increasing from the inner shells and the increase is quite high until they reach maxima at about shell number 20 or 21. Then they start falling although quite slowly. This can be understood from the fact that the points such as P are easily reached by the rays as the density of the electrons in these parts falls as $1/r^2$ and the radiation will not be attenuated as much as it would be along the axis OO′. The slight fall in S_T in the outermost shells is due to the fact that the incident beam itself is diluted by the $\cos\theta$ factor where θ is the angle between the radius vector and the path of the ray.

In Fig. 3(a), we have plotted S_T along OO′ direction corresponding to an increased incident radiation ($I = 10$). The results are quite different from those given in Fig. 2(a) for $I = 1$. The increased irradiation changes the variation of the source function. The quantity S_T along OO′ in this case keeps on increasing although there is a gradual flattening towards the outer layers of the atmosphere. The source function along QP direction with the increased irradiation (Fig. 3b) behaves very similar to that given in Fig. 2(b), but with enhanced magnitude.

The flux profiles are plotted in Fig. 4 for $I = 1$, 5 and 10. We have considerd a line with $x = \pm 5$ Doppler units and employed a Doppler profile. When there is no irradiation, we obtain lines with deep cores. When irradiation is introduced the flux in the lines is increased considerably at all points in the line. But the increase in flux in the cores (F_C) is considerably more than in the wings (F_W). For example in Fig. 4(a), the ratio F_W/F_C is about 25 when there is no irradiation (the dotted curve). But in the presence of irradiation this ratio reduces to 1.3–1.4 depending on the proximity of the secondary. Because of irradiation, the flux in the whole line is dramatically increased disproportionately, the cores benefitting more than the wings. The same phenomenon occurs when the strength of the incident beam is increased as shown in Figs 4(b) and (c). The equivalent width has been calculated by using the formula

$$W = \int_{-\alpha}^{+\alpha} (1 - F_x/F)dx \tag{3}$$

where F and F_x are the fluxes in the continuum and at a frequency x. α is the half band width of the line and is taken to be equal to 5 Doppler units. These equivalent widths are given in Table 1.

Table 1. The equivalent widths (W) in Doppler units. Equivalent width without reflection = 2.34. Note how the enhanced irradiation reduces the equivalent widths.

I \ r_1/R	1/2	1/3	1/4	1/5
1	0.61	0.65	0.67	0.68
5	0.16	0.17	0.18	0.18
10	0.08	0.09	0.10	0.10

In this paper, we have shown by a simple calculation, how the profiles of absorption lines change in a scattering medium with reflection. However, one should consider the temperature changes due to irradiation and also the effects of orbital revolution on the formation of spectral lines. This is under investigation.

References

Grant, I. P., Peraiah, A. 1972, *Mon. Not. R. astr. Soc.*, **160**, 239.
Napier, W. McD., Ovenden, M. W. 1970, *Astr. Astrophys.*, **4**, 129.
Peraiah, A. 1982, *J. Astrophys. Astr.*, **3**, 485 (Paper 1).
Peraiah, A. 1983a, *J. Astrophys. Astr.*, **4**, 11 (Paper 2).
Peraiah, A. 1983b, *J. Astrophys. Astr.*, **4**, 151 (Paper 3).
Peraiah, A., Rao, M. S. 1983, *J. Astrophys. Astr.*, **4**, 175 (Paper 4).
Young, R. K. 1922, *Pub. Dominion Astrophys. Obs.*, **1**, 105.